

Theoretical study of slab waveguide optical sensor with left-handed material as a core layer

SOFYAN A. TAYA^{1*}, TAHER M. EL-AGEZ¹, HANI M. KULLAB¹,
MAZEN M. ABADLA², MOHAMED M. SHABAT¹

¹Physics Department, Islamic University of Gaza, Gaza, Palestine

²Physics Department, Alaqsa University, Gaza, Palestine

*Corresponding author: staya@iugaza.edu.ps

A three-layer planar waveguide sensor consisting of thin left-handed material core layer is investigated for sensing applications. The sensitivity of the proposed sensor to the changes in the refractive index of the cladding is presented and studied for TE-polarized light. It is observed that the sensitivity of the proposed sensor is improved compared to that of the conventional three-layer slab waveguide sensor. It is also found that the sensitivity of the structure proposed is negative and critically dependent on the dispersive permittivity and permeability of the core layer.

Keywords: slab waveguides, optical sensors, left-handed material, sensitivity, power.

1. Introduction

Optical waveguide sensors have been used for analytical purposes for a number of years [1–6]. The sensing operation of the slab waveguide sensors is performed by the evanescent tail of the modal field in the cover medium (cladding). The guided electromagnetic field of the waveguide mode extends as an evanescent field into the cladding and the substrate media and senses an effective refractive index of the waveguide mode. The effective refractive index of the propagating mode depends on the structure parameters, *e.g.*, the guiding layer thickness and dielectric permittivity and magnetic permeability of the media constituting the waveguide. As a result, any change in the refractive index of the cladding results in a change in the effective refractive index of the guided mode. The basic sensing principle of the planar waveguide sensor is to measure the changes in the effective refractive index due to changes in the refractive index of the cladding [1]. Many theoretical and experimental studies have been conducted to improve the sensitivity of slab waveguide sensors.

TAYA *et al.* [7–10] proposed optical waveguide sensors in which one or both of the surrounding media have an intensity dependent refractive index. It is found that utilizing nonlinear media can enhance the sensitivity of slab waveguide sensors. Another class of optical waveguide sensors has been proposed with the so-called reverse symmetry design [11–13]. In these structures the substrate has a refractive index being less than that of the cladding medium. This design offers evanescent optical fields deeply penetrating into the cover sample analyzed. Therefore, the sensitivity has shown an improvement in the reverse symmetry configuration.

Slab waveguide sensors have been used for a wide range of applications such as on-line bacteria [14], and living cell monitoring [15], multidepth screening of living cells [16], detection of protein adsorption [17], lipid bilayers [18], and affinity binding [19].

Metamaterials are artificial media, in which man-made structural units play the role of atoms. Thus, the complex phenomena in metamaterials result from the characteristics of the individual elements as well as from the way they are arranged in a lattice. In other words, metamaterials gain emerging properties that were not available in their constitutive elements alone. This provides enormous flexibility in tailoring the response of metamaterials to external waves or fields. The history of these materials began with the paper of VESELAGO [20], who predicted a number of remarkable properties of waves in a material with simultaneously negative dielectric permittivity ϵ and magnetic permeability μ . Such media are usually termed as left-handed materials (LHMs), since the electric and magnetic fields form a left-handed set of vectors with the wave vector. Recent experimental demonstration of the novel composite material with a negative index refraction, opens up a unique possibility of designing novel types of devices, where electromagnetic waves do not propagate in a conventional way [21]. One of the first applications of LHMs was reported by PENDRY [22], who demonstrated that a slab of a lossless LHM can provide a perfect image of a point source. GRIBC and ELEFTHERIADES [23] verified by simulation the enhancement of evanescent waves in a transmission-line network by using a negative refractive index material. In 2003, it was shown that left-handed materials can enhance the evanescent field in planar slab waveguides [24]. Recently, left-handed materials have been proposed as a mechanism of building cloaking devices [25]. TAYA *et al.* proposed an optical slab waveguide sensor using LHM layer [6]. They showed that the sensitivity can be enhanced using LHMs in the field of optical evanescent sensors.

In this paper, bulk polaritons propagating along a slab waveguide with a lossy negative index material film are investigated. The dispersion relation and the sensitivity of the effective refractive index to variations in the refractive index of the cladding are derived. The power flowing in each layer of the structures proposed is also investigated. The variation of the sensitivity with the parameters of the proposed structure is presented. Goos–Hänchen shift and the penetration depth both in the cladding and the substrate layers are also presented.

2. Theory

We consider an asymmetric slab waveguide with an LHM layer occupying the region $0 < z < d$, which is characterized by an electric permittivity ϵ_2 and magnetic permeability μ_2 such that

$$\epsilon_2(\omega) = 1 - \frac{\omega_p^2}{\omega^2 + i\gamma\omega} \quad (1)$$

$$\mu_2(\omega) = 1 - \frac{F\omega^2}{\omega^2 - \omega_o^2 + i\gamma\omega} \quad (2)$$

where ω_p is the plasma frequency, ω_o is the resonance frequency, γ is the electron scattering rate, and F is the fractional area of the unit cell occupied by the split ring [26]. The slab is sandwiched between a dielectric cladding occupying the region $z > d$ with ϵ_3 and μ_3 and a dielectric substrate occupying the region $z < 0$ with ϵ_1 and μ_1 , as shown in Fig. 1.

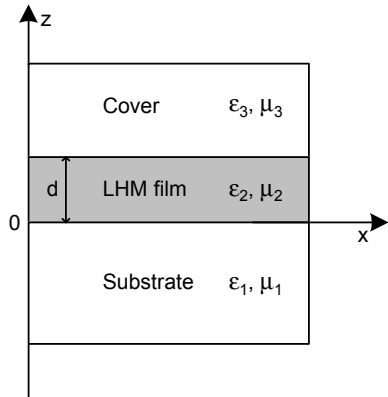


Fig. 1. Schematic diagram of a left-handed material slab sandwiched between two semi-infinite dielectric media.

The time harmonic electromagnetic fields in the region $z < 0$ are

$$\mathbf{E}_1(x, z) = \hat{y}A e^{\beta_1 z} e^{ik_x x} \quad (3)$$

$$\mathbf{H}_1(x, z) = \frac{A}{\omega\mu_0\mu_1} e^{\beta_1 z} (i\beta_1 \hat{x} + k_x \hat{z}) e^{ik_x x} \quad (4)$$

In the region $0 < z < d$, the fields are in the form

$$\mathbf{E}_2(x, z) = \hat{y} [B e^{ik_{z,2} z} + C e^{-ik_{z,2} z}] e^{ik_x x} \quad (5)$$

$$\mathbf{H}_2(x, z) = \frac{A}{\omega\mu_0\mu_2} \left[-Be^{ik_{z,2}z} (k_{z,2}\hat{x} - k_x\hat{z}) + Ce^{-ik_{z,2}z} (k_{z,2}\hat{x} + k_x\hat{z}) \right] e^{ik_x x} \quad (6)$$

For the region $z > d$,

$$\mathbf{E}_3(x, z) = \hat{y}D e^{-\beta_3(z-d)} e^{ik_x x} \quad (7)$$

$$\mathbf{H}_3(x, z) = -\frac{D}{\omega\mu_0\mu_3} e^{-\beta_3(z-d)} (i\beta_3\hat{x} - k_x\hat{z}) e^{ik_x x} \quad (8)$$

where \hat{x} , \hat{y} and \hat{z} are the unit vectors in x , y , and z directions, respectively. The constants A , B , C , D and the longitudinal propagation constant (k_x) are chosen to satisfy the boundary conditions. The relation between β_j ($j = 1, 2, 3$) and the normal vector component $k_{z,j}$ is given by

$$\beta_j = -ik_{z,j} = \pm \left(k_x^2 - \epsilon_j \mu_j k_0^2 \right)^{1/2} \quad (9)$$

where $k_x = k_0 N$, $k_0 = 2\pi/\lambda$, λ is the vacuum wavelength of the guided light, and N is the effective refractive index. It is worth noting that the sign of β_j should be shifted to the minus sign in the case where $\text{Re}(\epsilon_j\mu_j) > \text{Re}(N)$ [27].

The surface wave mode can be obtained with $k_{z,2}$ being replaced by $i\beta_2$. The boundary conditions require that the tangential components of \mathbf{E} and \mathbf{H} be continuous at $z = 0$ and $z = d$, yielding a set of homogeneous linear equations for the coefficients A , B , C , and D . The determinant of this set must be zero for nontrivial solution to exist. After some manipulations, the following equation, which is the bulk-polariton dispersion relation for TE waves, is obtained [26]

$$\left(\frac{k_{z,2}}{\mu_2} \right)^2 - \left(\frac{\beta_3}{\mu_3} + \frac{\beta_1}{\mu_1} \right) \frac{k_{z,2}}{\mu_2} \cot(k_{z,2}d) - \frac{\beta_3}{\mu_3} \frac{\beta_1}{\mu_1} = 0 \quad (10)$$

The sensitivity of the evanescent field sensor is defined as the change of the effective refractive index with respect to the change of the cladding refractive index n_3 , *i.e.*,

$$S = \frac{\partial N}{\partial n_3} \quad (11)$$

Differentiating the dispersion relation with respect to N yields

$$S = \frac{n_3}{N} \frac{\mu_3 k_{z,2}^2}{\beta_3(\mu_2^2\beta_3^2 + \mu_3^2 k_{z,2}^2)} \left[\frac{d}{\mu_2} + \frac{\mu_1(k_{z,2}^2 + \beta_1^2)}{\beta_1(\mu_2^2\beta_1^2 + \mu_1^2 k_{z,2}^2)} + \frac{\mu_3(k_{z,2}^2 + \beta_3^2)}{\beta_3(\mu_2^2\beta_3^2 + \mu_3^2 k_{z,2}^2)} \right]^{-1} \quad (12)$$

It is worthwhile to find the total time-averaged power transported by the waveguide,

$$P_{\text{total}} = \frac{k_x}{2\omega} \int_{-\infty}^{\infty} \frac{|E_y(z)|^2}{\mu_i(z)} dz \quad (13)$$

Therefore, the time-averaged power flowing in the substrate, the film, and the cladding layers are respectively given by

$$P_1 = \frac{k_x |A|^2}{4\omega \mu_0 \mu_3 \beta_1} \quad (14)$$

$$P_2 = \frac{k_x}{4\omega \mu_0 \mu_2} \left[\frac{|B|^2}{2k_{z,2}} \left(1 - e^{-2k_{z,2}d} \right) - \frac{|C|^2}{2k_{z,2}} \left(1 - e^{2k_{z,2}d} \right) + 2BCd \right] \quad (15)$$

and

$$P_3 = \frac{k_x |D|^2}{4\omega \mu_0 \mu_3 \beta_3} \quad (16)$$

It is instructive to study the percentage of time-averaged power contained in each region. To quantify the fractional power within the j -th layer, we define the film confinement factor Γ_j as

$$\Gamma_j = \frac{\text{Time - Average power transported in the } j\text{-th region}}{\text{Total time - Average power transported by the waveguide}} \quad (17)$$

The following relation must hold between the confinement factors

$$\sum_{j=1}^3 \Gamma_j = 1 \quad (18)$$

The effective waveguide thickness is an important factor in the dispersion of the effective refractive index and in the application of optical sensing. Knowing this, we calculate the effective waveguide thickness from the ray penetrations at the upper and lower boundaries of the guiding layer. The penetration of the guided wave from the guiding layer into the surrounding media can be written as

$$\lambda_1 = \frac{\mu_1 \mu_2}{\beta_1} \frac{k_{z,2}^2 + \beta_1^2}{\mu_2^2 \beta_1^2 + \mu_1^2 k_{z,2}^2} \quad (19)$$

$$\lambda_3 = \frac{\mu_3 \mu_2}{\beta_3} \frac{k_{z,2}^2 + \beta_3^2}{\mu_2^2 \beta_3^2 + \mu_3^2 k_{z,2}^2} \quad (20)$$

When a light beam undergoes a total internal reflection at the interface between two different media, the reflected light beam experiences a lateral shift in the plane of incidence from the position predicted by the geometrical optics because each plane wave component undergoes a different phase change [13]. This shift is known as Goos–Hänchen (GH) shift. GH-shifts at the film-substrate and the film-cladding interfaces are given by

$$GH_1 = \frac{\lambda}{\pi} \frac{\tan(\gamma)}{\sqrt{N^2 - n_1^2}} \quad (21)$$

$$GH_3 = \frac{\lambda}{\pi} \frac{\tan(\gamma)}{\sqrt{N^2 - n_3^2}} \quad (22)$$

with $\gamma = \sin^{-1}\left(\frac{N}{n_2}\right)$ being the angle of incidence.

3. Numerical results

Figure 1 shows the slab waveguide geometry under consideration. In the analysis below, we have assumed the wavelength of Nd:YAG laser $\lambda = 1064$ nm, the substrate to be SiO_2 with $n_1 = 1.5341$ ($\epsilon_1 = 2.35$), the cladding to be water of $n_3 = 1.33$ ($\epsilon_3 = 1.77$), and $\mu_1 = \mu_3 = 1$. Figures 2 and 3 show the variation of the real and imaginary parts of the sensitivity of the proposed sensor with the thickness of the LHM layer and the electron scattering rate γ . As can be seen from the figures, the sensitivity is negative and has a peak at a specific value of the guiding layer thickness d . It then decays towards lower values for high values of d due to the high field confinement.

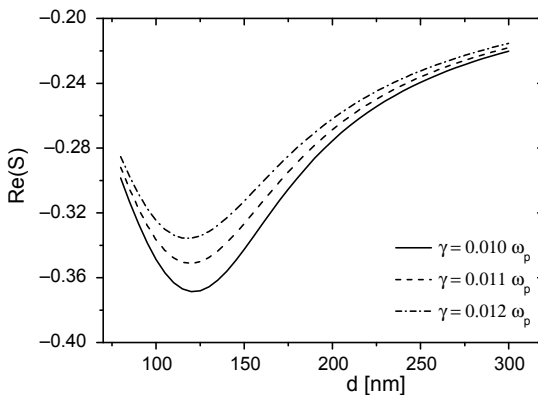


Fig. 2. The real part of the sensitivity of the proposed sensor versus the thickness of the guiding layer for different values of the electron scattering rate for $\lambda = 1064$ nm, $\epsilon_1 = 2.35$, $\epsilon_3 = 1.77$, $\mu_1 = \mu_3 = 1$, $\omega_p = 2\omega$, $\omega_o = 0.4\omega_p$, and $F = 0.56$.

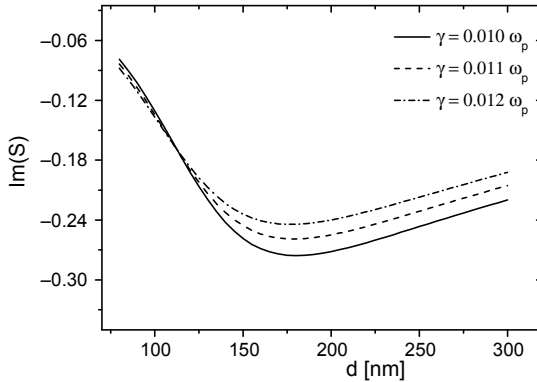


Fig. 3. The imaginary part of the sensitivity of the proposed sensor versus the thickness of the guiding layer for different values of the electron scattering rate for $\lambda = 1064$ nm, $\epsilon_1 = 2.35$, $\epsilon_3 = 1.77$, $\mu_1 = \mu_3 = 1$, $\omega_p = 2\omega$, $\omega_o = 0.4\omega_p$, and $F = 0.56$.

The absolute values of the real and imaginary parts of the sensitivity increase as γ decreases.

It is very important to compare the sensitivity of the proposed sensor to that of the conventional three-layer slab waveguide sensor with positive index guiding layer. Figure 4 shows the absolute value of the real part of the sensitivity of the proposed sensor and that of the conventional three-layer slab waveguide sensor with positive index material guiding layer. It is clear from the figure that the sensor proposed has an improved sensitivity. The improvement may be attributed to the property of amplification of evanescent waves observed in LHM [28].

The negative value of the sensitivity of the structure proposed is considered as a new feature that has not been observed in slab waveguide optical sensors. To clarify

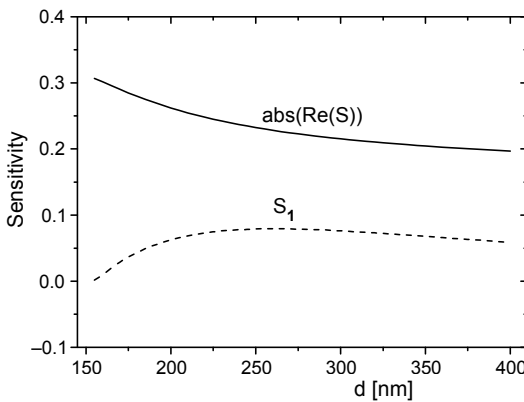


Fig. 4. Comparison between the sensitivity of the proposed sensor and that of the conventional sensor for $\lambda = 1064$ nm, $\epsilon_1 = 2.35$, $\epsilon_3 = 1.77$, $\mu_1 = \mu_3 = 1$, $\omega_p = 2\omega$, $\omega_o = 0.4\omega_p$, $\gamma = 0.012\omega_p$ and $F = 0.56$ (S_1 is the sensitivity of conventional structure).

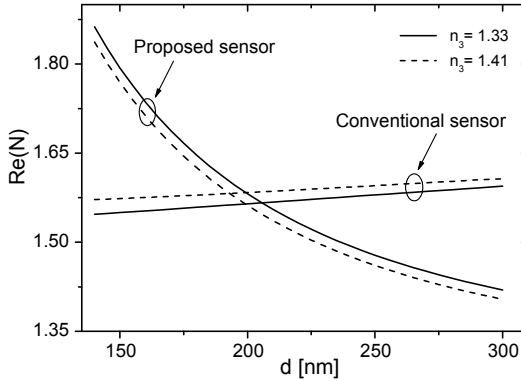


Fig. 5. The real part of the effective refractive index of the proposed sensor and that of the conventional sensor versus the thickness of the guiding layer for different values of the index of the cladding for $\lambda = 1064 \text{ nm}$, $\epsilon_1 = 2.35$, $\mu_1 = \mu_3 = 1$, $\omega_p = 2\omega$, $\omega_o = 0.4\omega_p$, $\gamma = 0.012\omega_p$ and $F = 0.56$.

At this point, we plot the real part of the effective refractive index as a function of d for different values of the cladding index. In the case of the proposed sensor, the effective refractive index N decreases as the cladding index n_3 increases, as shown in Fig. 5. This explains the negative value of the sensitivity which is the differentiation of N with respect to n_3 . For the conventional sensor, N increases as n_3 increases.

In Figures 6 and 7, the real and imaginary parts of the sensitivity are plotted versus the thickness of the guiding layer for different values of the fractional area of the unit cell occupied by the split ring. As can be seen from the figures, $\text{Re}(S)$ and $\text{Im}(S)$ exhibit

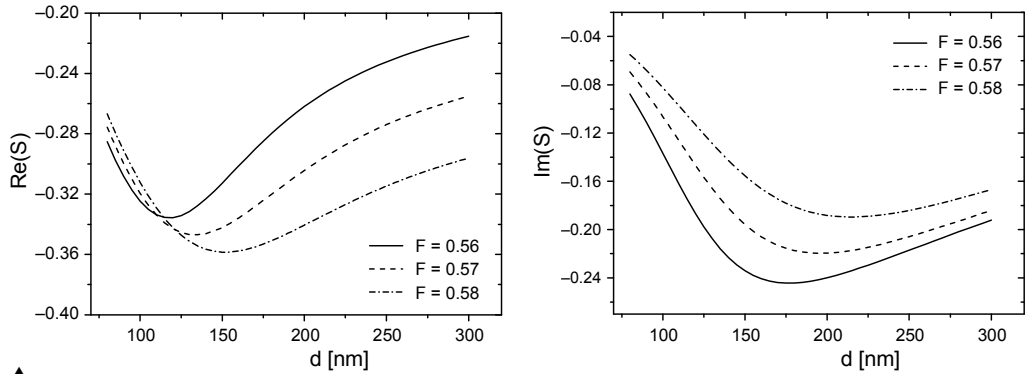


Fig. 6. The real part of the sensitivity of the proposed sensor versus the thickness of the guiding layer for different values of the fractional area of the unit cell occupied by the split ring for $\lambda = 1064 \text{ nm}$, $\epsilon_1 = 2.35$, $\epsilon_3 = 1.77$, $\mu_1 = \mu_3 = 1$, $\omega_p = 2\omega$, $\omega_o = 0.4\omega_p$, $\gamma = 0.012\omega_p$.

Fig. 7. The imaginary part of the sensitivity of the proposed sensor versus the thickness of the guiding layer for different values of the fractional area of the unit cell occupied by the split ring for $\lambda = 1064 \text{ nm}$, $\epsilon_1 = 2.35$, $\epsilon_3 = 1.77$, $\mu_1 = \mu_3 = 1$, $\omega_p = 2\omega$, $\omega_o = 0.4\omega_p$, $\gamma = 0.012\omega_p$.

different behaviors with varying F . Contrary to $\text{Im}(S)$, the absolute value of $\text{Re}(S)$ increases with increasing F for a given value of d .

Figures 8, 9, and 10 show the power transported in the substrate, the guiding film, and the cladding, respectively. Many interesting features can be observed in these figures. First, the powers transported in the substrate and the cladding show the same behavior with γ . Decreasing γ enhances both of the powers. The enhancement of $\text{Re}(P_3)$ with decreasing γ explains the improvement of $\text{Re}(S)$ with decreasing γ , as observed in Fig. 2. The sensitivity of evanescent field sensors is totally dependent on the power transported in the analyte medium (the material to be detected in the cladding

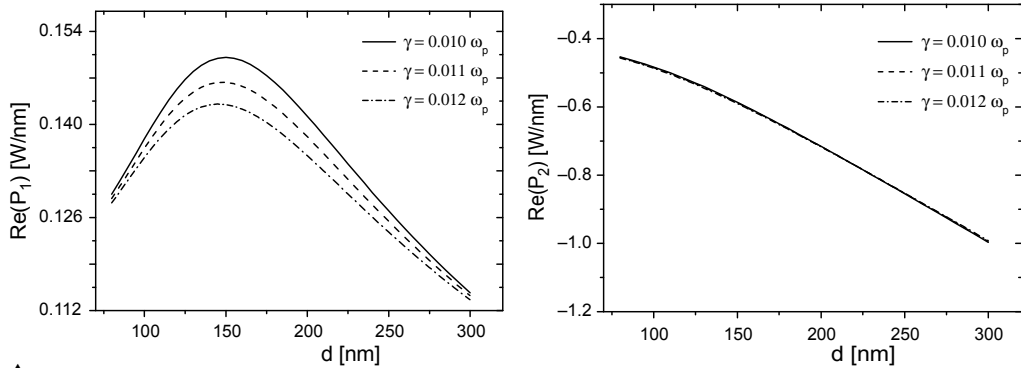


Fig. 8. The real part of the power flowing within the substrate layer versus the thickness of the guiding layer for different values of the electron scattering rate for $\lambda = 1064 \text{ nm}$, $\epsilon_1 = 2.35$, $\epsilon_3 = 1.77$, $\mu_1 = \mu_3 = 1$, $\omega_p = 2\omega$, $\omega_o = 0.4\omega_p$, and $F = 0.56$.

Fig. 9. The real part of the power flowing through the guiding layer versus the thickness of the core layer for different values of the electron scattering rate for $\lambda = 1064 \text{ nm}$, $\epsilon_1 = 2.35$, $\epsilon_3 = 1.77$, $\mu_1 = \mu_3 = 1$, $\omega_p = 2\omega$, $\omega_o = 0.4\omega_p$, and $F = 0.56$.

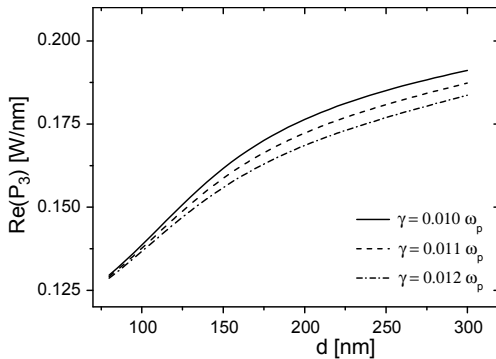


Fig. 10. The real part of the power flowing through the cladding layer versus the thickness of the guiding layer for different values of the electron scattering rate for $\lambda = 1064 \text{ nm}$, $\epsilon_1 = 2.35$, $\epsilon_3 = 1.77$, $\mu_1 = \mu_3 = 1$, $\omega_p = 2\omega$, $\omega_o = 0.4\omega_p$, and $F = 0.56$.

layer). Second, the negative value of the film power is the most important feature that can be seen in Fig. 9. This is one of the main differences between LHM and conventional materials. In LHM, the Poynting vector \mathbf{S} always forms a left-handed set with the vectors \mathbf{E} and \mathbf{H} . Accordingly, \mathbf{S} and the propagation vector \mathbf{k} are in opposite directions. Thus, it is clear that LHMs are substances with the so-called negative group velocity, which occurs in particular in anisotropic substances or when there is spatial dispersion. In brief, Fig. 9 emphasizes the fact that in LHMs the phase velocity is opposite to the energy flow. Third, the effect of γ on the power transported in the film is barely detectable in the range considered for γ due to the large value of $\text{Re}(P_2)$ compared to $\text{Re}(P_1)$ and $\text{Re}(P_3)$.

In order to study some additional parameters of the structure proposed, we plot the penetration depth and the GH shifts as a function of the guiding layer thickness for different values of the electron scattering rate γ , as shown in Figs. 11 and 12, respec-

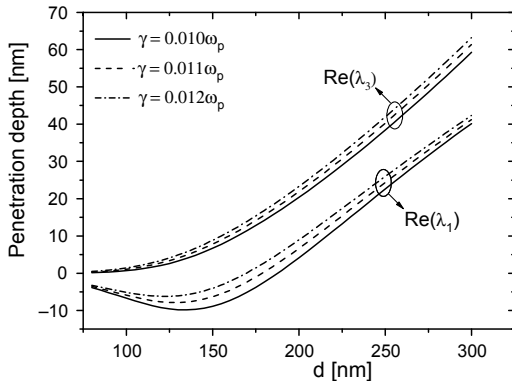


Fig. 11. The penetration depth in the substrate and the cladding layers versus the thickness of the guiding layer for different values of the electron scattering rate for $\lambda = 1064 \text{ nm}$, $\epsilon_1 = 2.35$, $\epsilon_3 = 1.77$, $\mu_1 = \mu_3 = 1$, $\omega_p = 2\omega$, $\omega_o = 0.4\omega_p$, and $F = 0.56$.

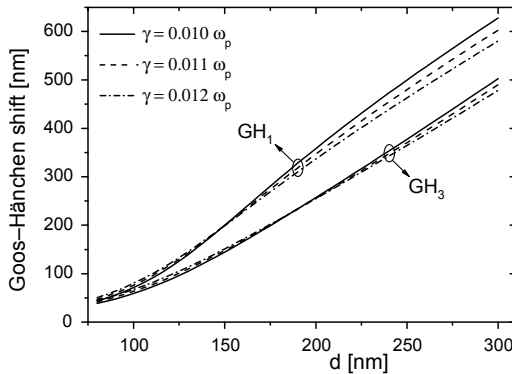


Fig. 12. The Goos–Hänchen shift in the substrate and the cladding layers versus the thickness of the guiding layer for different values of the electron scattering rate for $\lambda = 1064 \text{ nm}$, $\epsilon_1 = 2.35$, $\epsilon_3 = 1.77$, $\mu_1 = \mu_3 = 1$, $\omega_p = 2\omega$, $\omega_o = 0.4\omega_p$, and $F = 0.56$.

tively. Both of them can be treated as a probe for detecting changes in the refractive index of an aqueous cladding. In the above analysis, we have adopted the effective refractive index as a probe for detecting the cladding index changes which is one of the most commonly used techniques in slab waveguide sensors. Generally, any cladding-index dependent waveguide parameter can be used as the probe for optical sensing purposes, provided that this parameter is practically measurable. Both the penetration depth and the GH shift are dependent on the cladding index and are measurable. For example, several techniques have been developed for measuring the GH shift. BRETENAKER *et al.* investigated experimentally the measurement of the GH shift for only one reflection [29]. Their method uses the high sensitivity of the eigenstates of a quasi-isotropic laser to small perturbations to measure GH shift for angles of incidence both below and above the critical angle. Another approach was proposed to measure the GH shift [30] based on the modulation of the polarization state of a laser by an electro-optic modulator combined with a precise measurement of the resulting spatial displacement with a position-sensitive detector. The sensitivity of any waveguide parameter to changes in the cladding index is given as the differentiation of that parameter with respect to n_3 .

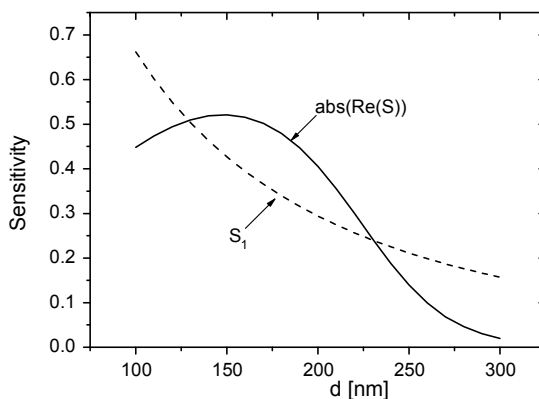


Fig. 13. Comparison between the real part of the sensitivity of the proposed sensor in a reverse-symmetry configuration and that of the conventional sensor S_1 for $\lambda = 1064$ nm, $\epsilon_1 = 1.00$, $\epsilon_3 = 1.77$, $\mu_1 = \mu_3 = 1$, $\omega_p = 2\omega$, $\omega_o = 0.4\omega_p$, $\gamma = 0$, and $F = 0.7$.

Finally, we investigate the behavior of the proposed sensor in reverse symmetry configuration because of the high sensitivity shown in the literature [11–13] for the conventional slab waveguide sensors in reverse symmetry. To achieve the reverse symmetry configuration, we assume the substrate to be air with $\epsilon_1 = 1.00$ and the cladding to be water of $\epsilon_3 = 1.77$. Figure 13 shows the absolute value of the real part of the sensitivity of the proposed sensor and the sensitivity S_1 of the conventional three-layer slab waveguide sensor both in reverse symmetry configuration. As can be seen from the figure the proposed sensor has an improved sensitivity in a specific range of the thickness of the guiding layer.

4. Conclusions

In this paper, we have proposed a three-layer slab waveguide optical sensor consisting of a left-handed material core layer. The sensitivity of the proposed sensor to the changes in the refractive index of the cladding is found to be enhanced using the negative index material guiding layer. Moreover, the sensitivity showed a critical dependence on the parameters of the LHM, which means that it can be maximized through proper choice of these parameters. LHMs of simultaneously negative and dispersive ϵ and μ are currently receiving high interest due to many potential applications. We believe that optical waveguide sensing is one of such applications.

References

- [1] TIEFENTHALER K., LUKOSZ W., *Sensitivity of grating couplers as integrated-optical chemical sensors*, Journal of the Optical Society of America B **6**(2), 1989, pp. 209–220.
- [2] PARRIAUX O., DIERAUER P., *Normalized expressions for the optical sensitivity of evanescent wave sensors*, Optics Letters **19**(7), 1994, pp. 508–510.
- [3] HORVATH R., SKIVESEN N., PEDERSEN H.C., *Measurement of guided light-mode intensity: An alternative waveguide sensing principle*, Applied Physics Letters **84**(20), 2004, pp. 4044–4046.
- [4] TAYA S.A., EL-AGEZ T.M., *Comparing optical sensing using slab waveguides and total internal reflection ellipsometry*, Turkish Journal of Physics **35**(1), 2011 pp. 31–36.
- [5] EL-AGEZ T., TAYA S., *Theoretical spectroscopic scan of the sensitivity of asymmetric slab waveguide sensors*, Optica Applicata **41**(1), 2011, pp. 89–95.
- [6] TAYA S.A., SHABAT M.M., KHALIL H.M., *Enhancement of sensitivity in optical waveguide sensors using left-handed materials*, Optik – International Journal for Light and Electron Optics **120**(10), 2009, pp. 504–508.
- [7] TAYA S.A., SHABAT M.M., KHALIL H.M., *Nonlinear planar asymmetrical optical waveguides for sensing applications*, Optik – International Journal for Light and Electron Optics **121**(9), 2010, pp. 860–865.
- [8] TAYA S.A., SHABAT M.M., KHALIL H.M., JÄGER D.S., *Theoretical analysis of TM nonlinear asymmetrical waveguide optical sensors*, Sensors and Actuators A **147**(1), 2008, pp. 137–141.
- [9] SHABAT M.M., KHALIL H.M., TAYA S.A., ABADLA M.M., *Analysis of the sensitivity of self-focused nonlinear optical evanescent waveguide sensors*, International Journal of Optomechatronics **1**(3), 2007, pp. 284–296.
- [10] KHALIL H.M., SHABAT M.M., TAYA S.A., ABADLA M.M., *Nonlinear optical waveguide structure for sensor application: TM case*, International Journal of Modern Physics B **21**(30), 2007, pp. 5075–5089.
- [11] HORVATH R., LINDVOLD L., LARSEN N., *Reverse-symmetry waveguides: Theory and fabrication*, Applied Physics B **74**(4–5), 2002, pp. 383–393.
- [12] HORVATH R., PEDERSEN H.C., LARSEN N.B., *Demonstration of reverse symmetry waveguide sensing in aqueous solutions*, Applied Physics Letters **81**(12), 2002, pp. 2166–2168.
- [13] TAYA S.A., EL-AGEZ T.M., *Reverse symmetry optical waveguide sensor using plasma substrate*, Journal of Optics **13**(7), 2011, article 075701.
- [14] DUDAK F.C., BOYACI I.H., *Rapid and label-free bacteria detection by surface plasmon resonance (SPR) biosensors*, Biotechnology Journal **4**(7), 2009 pp. 1003–1011.
- [15] YE FANG, FERRIE A.M., FONTAINE N.H., MAURO J., BALAKRISHNAN J., *Resonant waveguide grating biosensor for living cell sensing*, Biophysical Journal **91**(5), 2006 pp. 1925–1940.

- [16] HORVATH R., COTTIER K., PEDERSEN H.C., RAMSDEN J.J., *Multidepth screening of living cells using optical waveguides*, Biosensors and Bioelectronics **24**(4), 2008 pp. 799–804.
- [17] VÖRÖS J., *The density and refractive index of adsorbing protein layers*, Biophysical Journal **87**(1), 2004 pp. 553–561.
- [18] RAMSDEN J.J., *Partial molar volume of solutes in bilayer lipid membranes*, Journal of Physical Chemistry **97**(17), 1993, pp. 4479–4483.
- [19] DÜBENDORFER J., KUNZ R.E., *Compact integrated optical immunosensor using replicated chirped grating coupler sensor chips*, Applied Optics **37**(10), 1998 pp. 1890–1894.
- [20] VESELAGO V.G., *The electrodynamics of substances with simultaneously negative values of ϵ and μ* , Soviet Physics Uspekhi **10**(4), 1968, pp. 509–514.
- [21] ZI HUA WANG, ZHONG YIN XIAO, SU PING LI, *Guided modes in slab waveguides with a left handed material cover or substrate*, Optics Communications **281**(4), 2008, pp. 607–613.
- [22] PENDRY J.B., *Negative refraction makes a perfect lens*, Physical Review Letters **85**(18), 2000, pp. 3966–3969.
- [23] GRIBC A., ELEFTHERIADES G.V., *Growing evanescent waves in negative-refractive index transmission-line media*, Applied Physics Letters **82**(12), 2003, pp. 1815–1817.
- [24] DE-KUI QING, GANG CHEN, *Enhancement of evanescent waves in waveguides using metamaterials of negative permittivity and permeability*, Applied Physics Letters **84**(5), 2004, pp. 669–671.
- [25] ALU A., ENGHETA N., *Achieving transparency with plasmonic and metamaterial coatings*, Physical Review E **72**(1), 2005, article 016623.
- [26] KEUNHAN PARK, BONG JAE LEE, CEJI FU, ZHUOMIN M. ZHANG, *Study of the surface and bulk polaritons with a negative index metamaterial*, Journal of the Optical Society of America B **22**(5), 2005, pp. 1016–1023.
- [27] SKIVESEN N., HORVATH R., PEDERSEN H.C., *Optimization of metal-clad waveguide sensors*, Sensors and Actuators B **106**(2), 2005, pp. 668–676.
- [28] CHANGCHUN YAN, QIONG WANG, YIPING CUI, *Generating mechanism of the energy-stream loops for the evanescent waves in a left-handed material slab*, Optik – International Journal for Light and Electron Optics **121**(1), 2010, pp. 63–67.
- [29] BRETENAKER F., LE FLOCH A., DUTRIAUX L., *Direct measurement of the optical Goos–Hänchen effect in lasers*, Physical Review Letters **68**(7), 1992, pp. 931–933.
- [30] GILLES H., GIRARD S., HAMEL J., *A simple measurement technique of the Goos–Hänchen effect with polarization modulation and position sensitive detector*, Optics Letters **27**(16), 2002, pp. 1421–1423.

Received May 24, 2011
in revised form September 5, 2011